IJCRT.ORG ISSN : 2320-2882

INTERNATIONAL JOURNAL OF CREATIVE RESEARCH THOUGHTS (IJCRT)

An International Open Access, Peer-reviewed, Refereed Journal

Effect of gamma ray irradiation on structural and optical properties of SnO_2/rGO nanocomposite-pellets

[1]Jagat Pal Singh, [2]G.C Joshi

[1]Department of Physics, G.B Pant University of Agri. & Tech., Pantnagar, India
[2]RITL, G.B Pant University of Agri. & Tech., Pantnagar, India

Abstract: *γ-radiation is an electromagnetic radiation of the highest energy, highly penetrating and extremely high frequency . In present research work, SnO_2/rGO nanocomposites powder were synthesized via Co-precipitation technique and then pellets are formed by using hydraulic press machine. Samples (T0, T30, T60, T120, T240) are irradiated using a Co^{60} gamma source with the various irradiation doses (0 kGy, 30 kGy, 60 kGy, 120 kGy, 240 kGy). In this light, the irradiated samples were characterized by X-ray powder diffraction (XRD), UV-Vis spectroscopy and, Fourier transform Infrared microscopy (FTIR) to evaluate the effect of γ-ray irradiation on their microstructure and optical properties of nanocomposite-pellets. FTIR spectrum has been used to authenticate the formation of Sn-O-Sn and C=C bond indicated the existence of SnO_2 and rGO, also increase in γ-ray doses peak intensities increases confirms reduction in particle size. XRD results revealed that the strong increment in β corresponding to (101) planes of cassiterite SnO_2/rGO nanostructure. This is evident from higher doses results reduction in crystallite size (D) [1] and increment in lattice strain (ε). By Tauc plot analysis optical band-gap (OBG) were calculated, OBG of pristine SnO_2/rGO nanocomposite-pellets is 3.58 eV, for irradiated samples T30, T60, T120, and T240 is 3.28 eV, 3.25, 3.19, and 3.11 eV results that as the γ -ray doses increases OBG decreases. The formation of shallow impurity states were responsible for the reduction of Eg with the increases in γ -ray doses [2]. According to this study, the flaws created by irradiation have a significant influence in the structural and optical characteristics of nanocomposites-pellets. In future, this research work is very useful for optoelectronic, microelectronics and, gas sensing applications.*

Keywords: gamma ray, nanocomposites, graphene oxide, X-ray

I. INTRODUCTION

Cassiterite-type metal oxide nanoparticles have exclusive optical, magnetic and electronic properties [3]. Structure of cassiterite-type metal oxides is unique [4]. SnO_2 is belongs to cassiterite family having noble optical, magnetic and electronic properties. To date, SnO_2 is a primary application material for light sensors [5], supercapacitors [6], electronic industurity [7] and, sensors for oxidation detection and gas reduction [8]. Short wavelength and high energy γ -ray irradiation provides a handy approach for the synthesis and modification of materials that can take place at room temperature [9-11]. Metal oxides high dose irradiation results in the development of microscopic defects like as vacancies, defect clusters and disruptions. These flaws function as recombined centers when the produced carriers are trapped [12]. It is crucial to remember that the optical, electric and physical characteristics of materials are greatly affected by radiation exposure [13-15].

The purpose of this study, to examine the γ –ray irradiation effects at different doses (30 kGy, 60 kGy, 120 kGy, and 240 kGy) on the structural and optical characteristics of SnO_2/rGO nanocomposite pallets alongside characterized by X-ray diffraction (XRD), UV-visible spectroscopy (UV-Vis) and FT-IR techniques.

II. EXPERIMENTAL

2.1 METHOD & MATERIAL

Reduced graphene oxide (rGO) was synthesized by the modified Hammer's method. The prepared suitable volume (1% weight of $SnCl_4.5H_2O$) of rGO was ultrasonicated for 2 hours in 50 ml deionized water to obtain a homogeneous suspension. The SnO_2/rGO nanocomposites was synthesized by the co-precipitation method. To synthesize SnO_2/rGO, 1M solution of $SnCl_4.5H_2O$ is stirred for 15 minute in 50 ml double deionized (DDI) water for 10 minute, then the rGO suspension is added to the $SnCl_4.5H_2O$ solution, followed by magnetic stirring of the entire mixture for 15 minute. 5 ml PEG (MW=400) is added to the entire mixture for nanoparticle embolization. The resulting mixture was kept to be shaken by a magnetic stirrer at 400 rpm to form a uniform mixture. Aqueous 1 M solution of NaOH is added drop by drop to the prepared mixture to raise the PH to 12 by continuous stirring. On completion of the reaction, a thick precipitate is found at the bottom of the flask. The whole mixture was stirred for 3 hours at 50 °C at the temperature controlled magnetic stirrer. Precipitation was filtered and the nanoparticle was washed 4 times using DDI water and twice using ethanol (99% purity AR grade), precipitates to exclude impurities and chloride ions.

The precipitates extract from the centrifuged tubes and precipitate dried at 90°C in hot air oven for 18 hours, then collected and ground using a mortar pestle. Eventually, the synthesized powder was calcined at 500°C for 3 hours placing inside in muffle furnace, collect the prepared sample from the crucible.

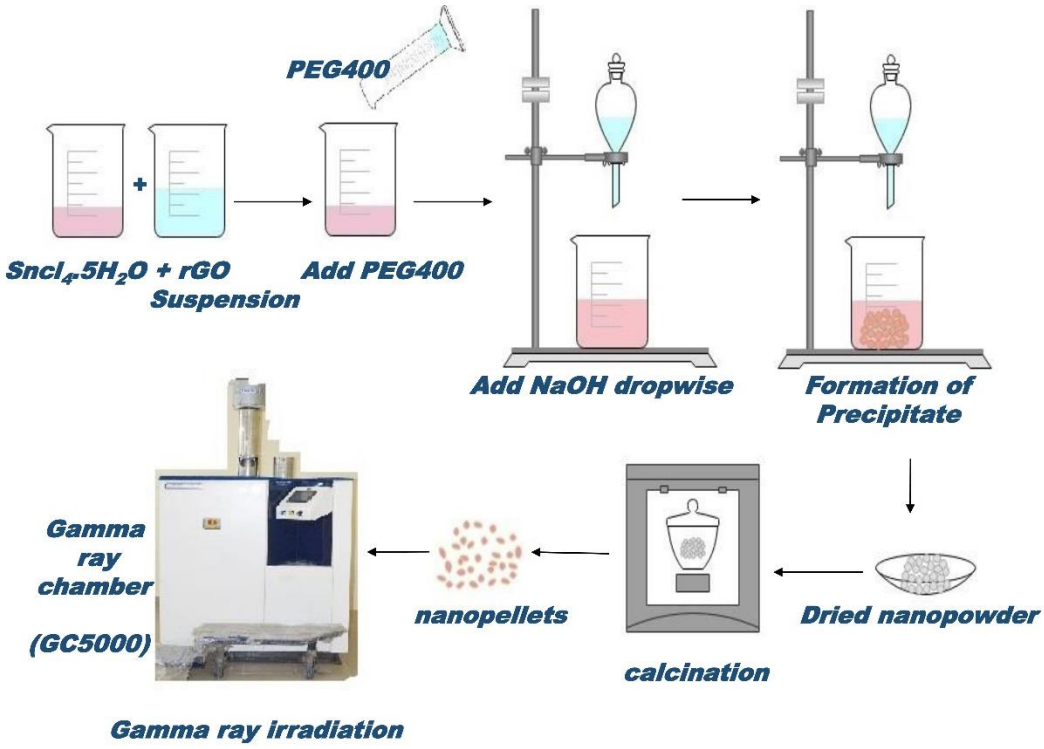

Figure 1. Scheme for Preparation of SnO_2/rGO nanocomposite-pellets and γ –ray irradiation.

2.2 GAMMA RAY IRRADIATION

For γ –ray irradiation studies, 13 milimeter (mm) diameter pellets were manufactured with a stainless steel die, by using a hydraulic pressing machine. The synthesized nanocomposites powder samples were pressed into pellet of 2 mm thick and 13 mm diameter and were taken in air tight polythene bags for irradiation. Gamma ray Chamber (model GC 5000 made by BRIT, Mumbai) installed in Radiation and Isotopic Tracers Laboratory, GBPUA&T, Pantnagar was used for irradiation of nanocomposite-pallet samples. Co^{60} (1.33 eV) used as a source of radioactive material in the lead shielded gamma chamber with dose of 30 kGy, 60 kGy, 120 kGy, and 240 kGy.

2.3 CHARACTERIZATION

The obtained nanocomposite-pellets were collected for characterization. Prepared samples was characterized by using XRD, FTIR, and UV-VIS techniques. The structural properties of SnO_2/rGO nanocomposites-pellets were studied by X-ray diffractometer measurements, XRD spectra have been done by using X'Pert Pro diffractrometer setup. The Cu-Kα radiation source (λ=1.5406 Å) operated at 40 kV with the scan rate of 5˚/min over the range of 10˚- 90˚. The spectral transmittance and absorbance measurements were obtained using UV-Vis spectrometer (model: LAMBDA 365, made: PerkinElmer) in the spectral range of 190 nm to 1100 nm. The X-intercept obtained to extrapolating the linear portion of the exponential curve from the graph of $(\alpha h\nu)^2$ vs photon energy (hv) is the bandgap energy of the material. Transmittance spectra has been recorded using FTIR (model: Nicolet-6700, made: Thermo Scientific)

III. RESULT

3.1 X-ray diffraction

The Figure 2. shows the XRD patterns of the synthesized SnO_2/rGO nanocomposite-pellets before and after γ –ray irradiation. where the peaks along the quaternary can be indexed to SnO_2. The cassiterite structure of SnO_2 is precisely matched with ICDD number 41–1445 and the absence of any unwanted peaks has not been confirmed by the presence of impurities. The peak of the highest intensity (101) is observed along the bottom. As shown in Figure 2, as the γ –ray dose is increased on the SnO_2/rGO nanocomposite-pellets, the FWHM of the diffraction peaks decreases [16]. The crystallite size of the samples is found to be in between 2.5nm – 4.5 nm respectively. On increasing the amount of irradiation it was also found that the XRD peak intensity of 120 kGy and 240 kGy irradiated SnO_2/rGO nanocomposite-pellets was increased after irradiation. These modifications induced in nanocomposite-pellets are strongly dependent on the radiation doses [17] and are responsible for the energy transfer and defect generation during the irradiation process.

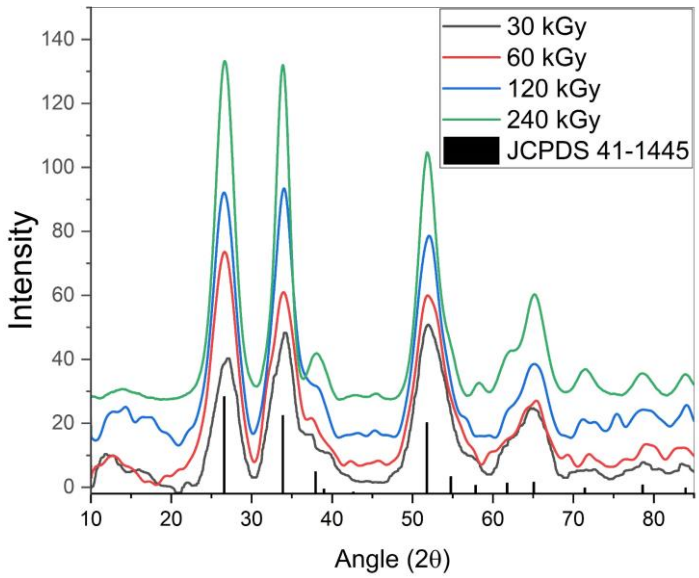

Figure 2. . XRD patterns of the samples T30, T60, T120, T240 which are irradiated with 30, 60, 120, and 240 kGy doses.

Crystallite size (D) were studied using the following formulae.

$$D = 0.9\lambda/\beta cos\theta \quad (1)$$

where, λ - Wavelength of radiation used, β - FWHM intensity of the diffraction peak, θ - Diffraction angle of the concerned diffraction peak.

It is also found that the XRD peaks become narrowing broader with increasing the γ –ray dose, which is responsible for increasing in the particle size of SnO_2 nanoparticles. This might be due to the poor growth of the nuclei when critical concentration of the spontaneous nucleation was reached [18]

3.2 UV-Vis Spectroscopy

Optical absorption techniques are one of the most prevailing and non-destructive methods used to estimate the optical properties of synthesized samples. Figure 3. below shows the UV-Visible spectra of the pristine and γ –ray irradiated SnO_2/rGO nanocomposites-pellet samples. The specific absorption peak in this region was found to be around 250-350 nm. The reason for the formation of shallow levels may be due to the formation of absorption bands inside the band gap due to doping [19]. The decrease in absorbance of the samples might be attributed to the development and accumulation of radiation-induced defects that serve as colour centres. With the aid of the absorption coefficient (α) and photon energy (hν), the energy band gap of pristine and γ –ray irradiated materials can be determined [20]

$$\alpha h\nu = A(h\nu - E_g)^n \quad (2)$$

Where A is a constant, E_g is OBG of the material and exponent n depends upon the direct and indirect allowed transition. In the present case, n is taken as ½ because of allowed direct transition.

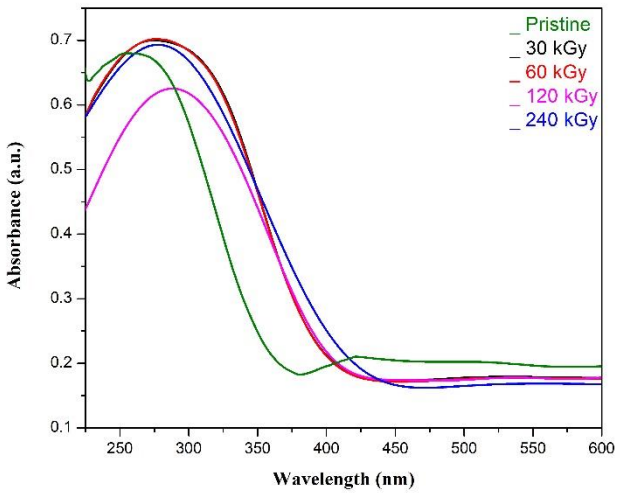

Figure 3. UV-Vis absorption spectra of Pristine and γ –ray irradiated SnO_2/rGO nanocomposite-pellets.

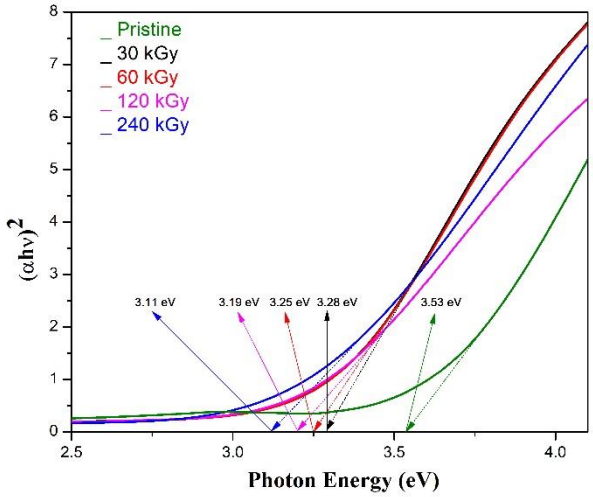

Figure 4. The plot of $(\alpha h\nu)^2$ vs hν for SnO_2/rGO nanocomposite-pellets.

The graph is extrapolated to the hν axis to calculate the value of OBG for the samples. As the dose of gamma radiations is increased, the bandgap spectra of SnO_2/rGO nanocomposites-pellets decreases from 3.53 eV to 3.11 eV. This increase is attributed to the improvement in crystallinity and packing density. This improvement in packing density and crystallinity is due to an increase in structural disorder, increase in defects at grain boundaries, and increase in lattice strain, which is a sign of good crystallinity. Pairs for electron-holes are generated as the energy transfer of radiation to the target atom results in the transfer of holes from the valence band to the conduction band. Free electrons and holes can move through the crystal until they are trapped by impurities, luminous centres, and other defects at some point during the irradiation. To maintain charge neutrality, electrons and holes are constantly reallocated to accessible electron and hole traps.

3.3 Fourier transform infrared spectroscopy (FTIR) analysis

The number of absorption peaks and the position of the bands depend on the chemical composition, morphology and crystalline structure [21]. FTIR technique is a more sensitive technique than XRD technique to know the phases and lattice distortions. Predicting the presence of certain functional groups is quite useful in the transmission mode of the FTIR technique, which are adsorbed at different frequencies, hence, revealing the structure of the material. The surface of the sintered samples at the wave number range of 400–4000 cm was analysed by FTIR to investigate the chemical clusters at room temperature. Several bands were visible in the wave number range 400 - 4000 cm−1. Of the isolated region, the peak area of 672 cm is assigned to the Sn–O–Sn vibrations, respectively [22].

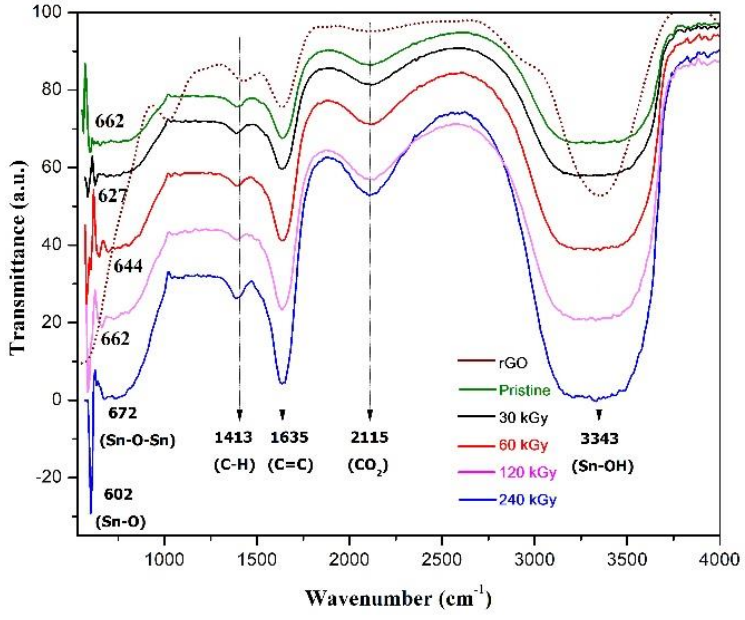

Figure 5. The IR spectra of rGO, Pristine and γ –ray irradiated SnO_2/rGO nanocomposite-pellets with the doses of 30, 60, 120, 240 kGy

The reduced graphene oxide (rGO) sample peak at 1033 cm^{-1} is due to CO binding, the peak at 1413 cm^{-1} and 1635 cm^{-1} is due to the presence of carbon in the rGO sample due to the C=H and C = C modes. The existence of hydrogen bonds causes strong and broad peaks around 3343 cm^{-1} to form O-H oscillators, which is due to the absorption of water molecules by the sample. A strong peak extending from 3500 cm^{-1} to 2500 cm^{-1} indicates the involvement of hydrogen bonds in the O–H oscillators, which may be

due to the Sn–OH group formed by the absorption of water. The presence of rGO in the sample is confirmed due to the C–H and C = C modes present at the peak at 1387 cm^{-1} and 1635 cm^{-1}. The absorption of CO_2 is confirmed by a weak absorption peak visible at 2117 cm^{-1} in the ambient atmosphere [23]. The peak appears at 585 cm^{-1} and 627 cm^{-1} due to the Sn–O stretching mode of vibration and the Sn–O–Sn anti-symmetric mode of vibration for sample T30. As the γ –ray dose is increased to 60 kGy, 120kGy and 240 kGy, the peak is shifted towards higher wave numbers at 644 cm^{-1}, 662 cm^{-1} and 672 cm^{-1}. In the samples, the γ –ray dose increases the peak intensity for the Sn-O stretching modes at 585 cm-1, 581 cm-1, 588 cm-1, and 602 cm-1. The position of the absorption band changes by the γ –ray (see inset of Figure 4). The observed changes in the size, width and position of the FTIR peaks are attributed to variations in local defects, grain size and nanoparticle size [24]. An increase in band intensity and bandwidth indicates a decrease in particle size [25].

IV. CONCLUSION

In this research work, we have synthesized SnO_2/rGO nanocomposite nanopowder by co-precipitation method and fabricated nanopellets with 13 mm diameter and 2 mm thickness using hydraulic press machine. The SnO_2/rGO nanopellets were irradiated by γ –ray of 30 kGy, 60 kGy, 120 kGy, and 240 kGy doses. The XRD spectra reveal that, using γ –ray irradiation techniques, the crystallite size of the nanoparticles is reduced and various effects such as increased microscopic strain are also produced. FTIR analysis shows strong bridge functional group in all samples confirming that SnO_2/rGO nanoparticles are formed. As the gamma ray dose increases, the optical absorption peak appears to shift towards the higher wavelength range, with the results of Tauc plot analysis showing that as the γ –ray doses on the nanocomposites-pellets is increased, The optical direct band gap is reduces. Hence from this, we can conclude that γ –ray irradiation of suitable dose can help us to enhance the structural and optical properties of SnO_2/rGO. In the future, this research work may be very useful for microelectronics, optoelectronics and low temperature gas sensing applications.

ACKNOWLEDGEMENT

The authors are thankful for the Incharge RITL, GBPUA&T Pantnagar for providing the facility for γ –ray irradiation.

Reference

[1] Abhirami, K. M., Sathyamoorthy, R., & Asokan, K. 2013. Structural, optical and electrical properties of gamma irradiated SnO thin films. *Radiation physics and chemistry*, *91*, 35-39.

[2] Pervez, M. F., Mia, M. N. H., Hossain, S., Saha, S. M. K., Ali, M. H., Sarker, P., ... & Chowdhury, M. A. M. 2018. Influence of total absorbed dose of gamma radiation on optical bandgap and structural properties of Mg-doped zinc oxide. *Optik*, *162*, 140-150.

[3] Thenmozhi C, ManivannanV, KumarE, & VeeraRethinaMurugan S. 2015. SYNTHESIS AND CHARACTERIZATION OF SnO2 AND PANI DOPED SnO2 NANOPARTICLES BY MICROWAVE ASSISTED SOLUTION METHOD. *International Research Journal of Engineering and Technology*, *August*. www.irjet.net

[4] Yang, Y., Wang, Y., & Yin, S. 2017. Oxygen vacancies confined in SnO 2 nanoparticles for desirable electronic structure and enhanced visible light photocatalytic activity. *Applied Surface Science*, *420*, 399–406. https://doi.org/10.1016/j.apsusc.2017.05.176

[5] Shaikh, S. K., Inamdar, S. I., Ganbavle, V. V., & Rajpure, K. Y. 2016. Chemical bath deposited ZnO thin film based UV photoconductive detector. *Journal of Alloys and Compounds*, *664*, 242–249. https://doi.org/10.1016/j.jallcom.2015.12.226

[6] Sasirekha, C., Arumugam, S., & Muralidharan, G. 2018. Green synthesis of ZnO/carbon (ZnO/C) as an electrode material for symmetric supercapacitor devices. *Applied Surface Science*, *449*, 521–527. https://doi.org/10.1016/j.apsusc.2018.01.172

[7] Rajwali, K., & Ming-Hu, F. 2015. Dielectric and magnetic properties of (Zn, Co) co-doped SnO2 nanoparticles. *Chinese Physics B*, *24*(12), 127803. 10.1088/1674-1056/24/12/127803/meta

[8] Wang, Z., Sackmann, A., Gao, S., Weimar, U., Lu, G., Liu, S., Zhang, T., & Barsan, N. 2019. Study on highly selective sensing behavior of ppb-level oxidizing gas sensors based on Zn2SnO4 nanoparticles immobilized on reduced graphene oxide under humidity conditions. *Sensors and Actuators, B: Chemical*, *285*(January), 590–600. https://doi.org/10.1016/j.snb.2019.01.109

[9] Chen, S., Liu, Y., & Wu, G. 2005. Stabilized and size-tunable gold nanoparticles formed in a quaternary ammonium-based room-temperature ionic liquid under γ-irradiation. *Nanotechnology*, *16*(10), 2360–2364. https://doi.org/10.1088/0957-4484/16/10/061

[10] Shin, H. S., Yang, H. J., Kim, S. Bin, & Lee, M. S. 2004. Mechanism of growth of colloidal silver nanoparticles stabilized by polyvinyl pyrrolidone in γ-irradiated silver nitrate solution. *Journal of Colloid and Interface Science*, *274*(1), 89–94. https://doi.org/10.1016/j.jcis.2004.02.084

[11] Henglein, A. 2001. Reduction of Ag(CN)2- on silver and platinum colloidal nanoparticles. *Langmuir*, *17*(8), 2329–2333. https://doi.org/10.1021/la001081f

[12] Merdrignac, O. M., Moseley, P. T., Peat, R., Sofield, C. J., & Sugden, S. 1992. The modification of gas-sensing properties of semiconducting oxides by treatment with ionizing radiation. *Sensors and Actuators: B. Chemical*, *7*(1–3), 651–655. https://doi.org/10.1016/0925-4005(92)80380-G

[13] Clough, R. L. 2001. High-energy radiation and polymers: A review of commercial processes and emerging applications. *Nuclear Instruments and Methods in Physics Research, Section B: Beam Interactions with Materials and Atoms*, *185*(1–4), 8–33. https://doi.org/10.1016/S0168-583X(01)00966-1

[14] Ibrahim, A. M., & Soliman, L. I. 1998. Effect of γ-irradiation on optical and electrical properties of Se(1 - (x))Te(x). *Radiation Physics and Chemistry*, *53*(5), 469–475. https://doi.org/10.1016/S0969-806X(98)00016-4

[15] Atanassova, E., Paskaleva, A., Konakova, R., Spassov, D., & Mitin, V. F. 2001. Influence of γ radiation on thin Ta2O5-Si structures. *Microelectronics Journal*, *32*(7), 553–562. https://doi.org/10.1016/S0026-2692(01)00043-X

[16] Fairose, S., Ernest, S., & Daniel, S. 2018. Effect of Oxygen Sputter Pressure on the Structural, Morphological and Optical Properties of ZnO Thin Films for Gas Sensing Application. *Sensing and Imaging*, *19*(1), 1–18. https://doi.org/10.1007/s11220-017-0184-5

[17] Waikar, M. R., Shaikh, A. A., & Sonkawade, R. G. 2019. The supercapacitive performance of woollen-like structure of CuO thin films prepared by the chemical method. *Vacuum*, *161*, 168-175. **https://doi.org/10.1016/j.vacuum.2018.12.034.**

[18] Qin, L., Xu, J., Dong, X., Pan, Q., Cheng, Z., Xiang, Q., & Li, F. 2008. The template-free synthesis of square-shaped SnO2 nanowires: The temperature effect and acetone gas sensors. *Nanotechnology*, *19*(18). https://doi.org/10.1088/0957-4484/19/18/185705

[19] Nachiar, R. A., & Muthukumaran, S. 2019. Structural, photoluminescence and magnetic properties of Cu-doped SnO2 nanoparticles co-doped with Co. *Optics and Laser Technology*, *112*(November 2018), 458–466. https://doi.org/10.1016/j.optlastec.2018.11.055

[20] Sangeetha, R., Muthukumaran, S., & Ashokkumar, M. 2015. Structural, optical, dielectric and antibacterial studies of Mn doped Zn0.96Cu0.04O nanoparticles. *Spectrochimica Acta - Part A: Molecular and Biomolecular Spectroscopy*, *144*, 1–7. https://doi.org/10.1016/j.saa.2015.02.056

[21] Ashokkumar, M., & Muthukumaran, S. 2014. Microstructure, optical and FTIR studies of Ni, Cu co-doped ZnO nanoparticles by co-precipitation method. *Optical Materials*, *37*(C), 671–678. https://doi.org/10.1016/j.optmat.2014.08.012

[22] Sharma, A., Varshney, M., Kumar, S., Verma, K. D., & Kumar, R. 2011. Magnetic properties of Fe and Ni doped SnO2 nanoparticles. *Nanomaterials and Nanotechnology*, *1*(1), 29–33. https://doi.org/10.5772/50948

[23] Yuan, Y., Jiang, Q., Yang, J., & Feng, L. 2016. Variation in luminescence and bandgap of Zn-doped SnO 2 nanoparticles with thermal decomposition. *Journal of Materials Science: Materials in Electronics*. https://doi.org/10.1007/s10854-016-5006-3

[24] Jouhannaud, J., Rossignol, J., & Stuerga, D. 2008. Rapid synthesis of tin (IV) oxide nanoparticles by microwave induced thermohydrolysis. *Journal of Solid State Chemistry*, *181*(6), 1439–1444. https://doi.org/10.1016/j.jssc.2008.02.040

[25] Srinivas, K., Rao, S. M., & Reddy, P. V. 2011. Structural, electronic and magnetic properties of Sn0.95Ni 0.05O2 nanorods. *Nanoscale*, *3*(2), 642–653. https://doi.org/10.1039/c0nr00597e